Catalysis Today 144 (2009) 258–264

Contents lists available at ScienceDirect

Catalysis Today

journal homepage: www.elsevier.com/locate/cattod

Effect of mass transfer on the reaction rate in a monolithic catalyst with porous walls

O.P. Klenov [a], S.A. Pokrovskaya [a,b,*], N.A. Chumakova [a,b], S.N. Pavlova [a], V.A. Sadykov [a,b], A.S. Noskov [a]

[a] Boreskov Institute of Catalysis, Siberian Branch of the Russian Academy of Sciences, pr. Lavrentieva 5, 630090 Novosibirsk, Russia
[b] Novosibirsk State University, ul. Pirogova, 630090 Novosibirsk, Russia

ARTICLE INFO

Article history:
Available online 10 January 2009

Keywords:
Monolithic catalyst
Porous wall
Reaction rate
Computational fluid dynamics

ABSTRACT

The influence of reacting gas flow on the heterogeneous reaction in catalyst volume of honeycomb porous monolith with triangular channels was studied. The spatial distributions of the reacting gas flow, the rates of local mass transfer between channel walls and gas flow, as well as the interaction of transfer processes and a catalytic reaction were determined on the basis of the computational fluid dynamics. The reactions of deep oxidation and steam reforming of methane were considered as model reactions.

It was shown that there is no stabilization of the reacting flow over the whole channel length under studied conditions. The most intensive changing of the gas streams appears near the channel inlet, which causes the highest local rates of interphase exchange processes, the rate difference is up to two orders of magnitude. A higher reaction rate exists in the initial part due to penetration of feed components into the catalyst volume through the frontal surface. This leads to increasing the effectiveness factor whose value is above unity near the channel inlet. The reaction rate limitation by the transport of reagents inside porous wall was observed along the monolith length.

1. Introduction

Ever-growing interest in structured catalyst systems is related with many new promising applications. New monolithic catalyst systems provide both the improvement of existing technologies and the development of new compact installations, in particular, for hydrogen energy technologies, production of liquid fuels from natural and oil gas of remote deposits, etc. [1–4]. To find a new design solution or conditions for an optimal operation mode, the detailed data concerning the effects of the mass and heat transfer on the catalytic reaction rates are necessary. This question is of special importance for catalytic processes occurring at high temperatures and short contact times, such as fuel combustion and selective hydrocarbons oxidation to synthesis gas.

Many studies are devoted to the problem of adequacy of mathematical description used for numerical studies of the processes in monolith channels. The correlations for the interphase transport processes between the catalyst wall and gas flow in the form of Nusselt and Sherwood numbers are widely and successfully used for description of processes in monolith channels of different shapes both in numerical simulations and chemical engineering practice. Nevertheless, the use of simplified plug-flow or boundary-layer models does not always allow the reveal of all features of hydrodynamic processes in a monolith catalyst system. In lumped models, some average values of temperature and concentration are considered instead of cross-sectional distributions, and transverse diffusive transport of mass and heat is estimated via global coefficients [5–9].

More precise analysis becomes possible on the base of computational fluid dynamics (CFD) modeling, which allows the using of complete mathematical models that consider the three-dimensional Navier–Stokes equations to account for the axial and radial transfer of mass, impulse, and energy in monoliths with channels of different shapes. In a series of studies, Deutschmann et al. [10–13] developed a modern multi-dimensional approach of detailed modeling the transfer processes and kinetics of chemical transformations as well. In particular, a critical evaluation of plug-flow, boundary-layer and general three-dimensional models for simulating the steady-state transport processes and chemistry in a honeycomb channel is given in [10].

The studies of catalytic processes using three-dimensional CFD modeling are carried out for washcoat monolithic systems where a ceramic monolith made of a support substrate (for example, cordierite) is pre-coated with a secondary support (alumina) and a catalytic active component. The two models are used: either the heterogeneous reaction is assumed to proceed on the outer surface

* Corresponding author at: Boreskov Institute of Catalysis, Siberian Branch of the Russian Academy of Sciences, pr. Lavrentieva 5, 630090 Novosibirsk, Russia. Tel.: +7 383 3269430; fax: +7 383 3306878.
E-mail address: pokrov@catalysis.ru (S.A. Pokrovskaya).

0920-5861/$ – see front matter © 2008 Elsevier B.V. All rights reserved.
doi:10.1016/j.cattod.2008.11.014

Nomenclature

c_{CH_4}, c_{O_2}	concentrations of methane and oxygen, correspondingly (gmol/cm^3)
k_1, k_2	rate constants of methane oxidation and steam reforming, correspondingly (cm^3/(gmol s))
P	channel perimeter (mm)
r_1, r_2	rates of methane oxidation and steam reforming, correspondingly (gmol/(cm^3 s))
S_0	area of catalyst cross-section (mm^2)
S_n	area of elementary channel surface (mm^2)
V_n	elementary volume (mm^3)
W	feed rate (l/h)
X	current length of monolith fragment or reactor (mm)

Greek letters

δ	wall thickness (mm)
η	effectiveness factor of catalyst porous volume

of the channel (this is taken in the boundary conditions) or the reaction-diffusion model is considered along the thickness of the washcoat to evaluate the gradients of the reacting substances inside the catalytic active layer. As for the catalyst monoliths prepared with porous supports such as α-Al_2O_3, it is necessary to account for the active component distribution in the whole volume of the porous catalyst structure [4].

In this work, the results of studies of the mass transfer in a catalyst with triangular channels, where the catalytic reaction at short contact times takes place inside the porous walls of the catalyst structure, are presented. The detailed distribution of the reacting gas flow in the system, the rate of local mass transfer between the channel walls and the gas flow, as well as the influence of mass transfer processes on the reaction rate were studied. CFD modeling of the gas flow under conditions of the catalytic reaction is carried out with the Fluent software.

The main goals of these studies are:

- Modeling and visualization of the gas flow in the porous honeycomb catalyst with the triangular channels under the conditions of the catalytic reaction.
- Evaluation of the impact of aerodynamics on the reaction rates.

2. Modeling approach

2.1. Catalyst monolith and reactor model

Studies were performed for a monolithic catalyst based on a honeycomb α-Al_2O_3 support with triangular straight channels, when the catalytic reaction proceeds inside the volume of porous structure. The catalyst shape corresponds to a real catalytic system developed at the Boreskov Institute of Catalysis for the partial oxidation of hydrocarbons at short contact times [14]. The catalysts with LaNiPt/CeO_2–ZrO_2 active component were successfully tested out in the partial oxidation of natural gas and the processes of reforming and selective oxidation of the liquid hydrocarbons (isooctane, benzine) into syngas as well. Typical samples of such honeycomb monoliths are presented in Fig. 1. The geometric and textural characteristics of α-Al_2O_3 used in simulations are given in Table 1.

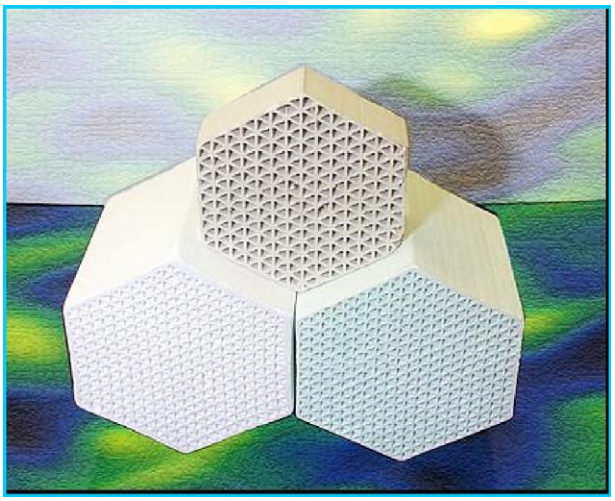

Fig. 1. Typical catalysts based on α-Al_2O_3 monoliths.

Since every channel within monolith structure behaves essentially alike, it is possible to analyze one channel [10,15]. For the purpose, fragments of a monolithic catalyst in the form of a separate triangular channel were considered. The scheme of the tube reactor with the honeycomb catalyst fragment is presented in Fig. 2. The reacting mixture consumption W was fed in the empty volume in front of the catalyst. The gas flow goes through the fragment of the honeycomb monolith and leaves the reactor. The walls of the catalyst have a porous structure whose volume is also permeable for the reacting flow. The insulation between the catalyst particle and the reactor wall is a solid medium impermeable for the flow. Accounting for the fact that the catalytic channel is narrow, the flow was assumed to be essentially laminar. The variants were analyzed when the fragment of 10 or 20 mm length was placed into the reactor of inner diameter of 4 mm; the distance between the reactor inlet and the front face of the monolith was 15 mm, while the length of the empty zone after the catalyst was 20 mm [16].

2.2. Mathematical description

The stationary flow of the gaseous reacting mixture was investigated in the tube reactor placed into a thermostat. The model discussed here is based on the Fluent software [17]. The system of three-dimensional Navier–Stokes equations including impulse, energy, and mass balances was used for description of the reacting flow in the volumes both of gas phase in the channel and the porous catalytic wall, as well as in the empty volumes before and after the catalyst fragment. The axial and transversal heat and mass transfer were taken into account.

The computation domain consists of the three subdomains (see Fig. 2):

(1) the empty volume inside the reactor (the complete Navier–Stokes equations are used here);

Table 1
Characteristics of α-Al_2O_3 monolithic substrate.

Channel form	Triangular
Wall thickness	0.3 mm
Triangle side	2.3 mm
Specific surface	3 m^2/g
Average pore diameter	72 nm
Pore volume	0.27 cm^3/g
Porosity	0.4

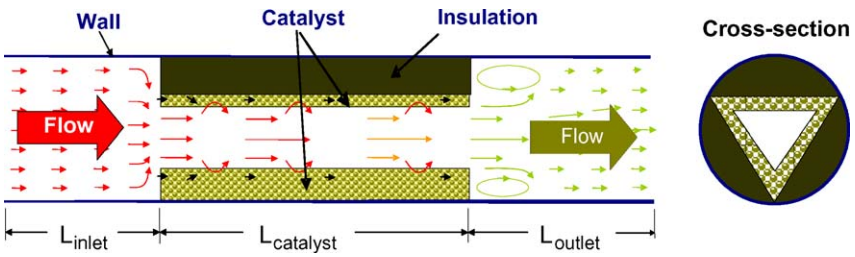

Fig. 2. The scheme of a tube reactor.

(2) the porous volume which is the catalyst structure (a quasi-homogeneous model in the form of the Navier–Stokes equations is used here as well, but with partially permeable media and under conditions of catalytic reactions; the pressure drop is calculated by the Ergun equation whose coefficients, both the viscous and dynamical terms, were estimated from the experimental data);
(3) the thermal insulation around the catalyst fragment (the energy conservation law is the only equation valid here accounting for the conductivity of the insulation).

The physico-chemical properties of the gas mixture and the solid phase are calculated using the Fluent software (database and the subroutines for calculating the properties of a mixture) and the data reported in the literature. In this work only heterogeneous catalytic reactions were considered. A uniform distribution of the active component in the volume of the catalyst porous wall is assumed, and the reaction rate is calculated for the volume of each cell of the numerical grid in the second subdomain.

The reaction of deep methane oxidation is considered as the main model reaction. To calculate the reaction rate according to this route, the following kinetic equation was used as an approximation for the more complex dependence obtained in [18]:

$$CH_4 + 2O_2 \rightarrow CO_2 + 2H_2O, \quad r_1 = k_1 c_{CH_4} c_{O_2}, \tag{1}$$

where c_j is the concentration of the jth component of the reacting mixture, and r_1 is the reaction rate.

The impact of aerodynamics of the gas flow was also studied for the methane steam reforming, which is one of the reforming reactions that proceed under interaction of methane with the products of methane oxidation. This pathway was considered as an example of reaction with the catalyst activity lower as compared to that for the methane oxidation. The reaction rate was described according to the equation of [19]:

$$CH_4 + H_2O \leftrightarrow CO + 3H_2,$$
$$r_2 = k_2 c_{CH_4} c_{H_2O} \left(1 - \frac{c_{CO} c_{H_2}^3}{c_{CH_4} c_{H_2O}} \frac{1}{K_{eq}}\right), \tag{2}$$

where c_j is the concentration of the jth component of the reacting mixture, r_2 is the 2nd reaction rate.

The simulation runs were carried out for modeling the system under atmospheric pressure at feed gas temperature of 988 K. The thermostat temperature was fixed at 988 K around the empty zone before the catalyst fragment and at 973 K along the fragment and after that. The inlet reaction mixture was fed with the rate of 18 l/h, which corresponds to the contact time of 5 ms. In order to avoid high heating and separate out the mass transfer effect, the low concentrations of reagents were taken, 3.3 vol% of methane and 1.55 vol% of oxygen.

The tool of CFD simulation is Fluent software, version 6.1 [17]. A finite-volume approach is implemented to solve the stationary boundary value problem under consideration. The spatial resolution was adapted to the aerodynamic conditions and the gradients of solution. We ran the computations both on the personal workstation and on the super-computer of the Siberian Super-Computer Center of the Siberian Branch of the Russian Academy of Sciences (Novosibirsk).

The following studies were performed:

- determination of gas flow velocity distribution near the inlet, in the catalyst channel and after the channel outlet;
- study of local mass transfer rates between the catalyst channel surface and the reacting gas flow;
- evaluation of the influence of aerodynamics on the rate of chemical transformation;
- determination of the efficiency of the catalyst porous volume in the reaction.

3. Results and discussion

3.1. Temperature distribution

As it was pointed above, the model includes the impulse, energy, and mass balances. Many factors, such as aerodynamic conditions, temperature distribution, local gas mixture composition, etc., influence the system behavior. In this paper the results of the first stage of studies are presented, and an attempt is made to clarify the effect of mass transfer on the reaction rate. For the purpose, at the fixed values of all above mentioned parameters the effect of the temperature inhomogeneity was minimized because

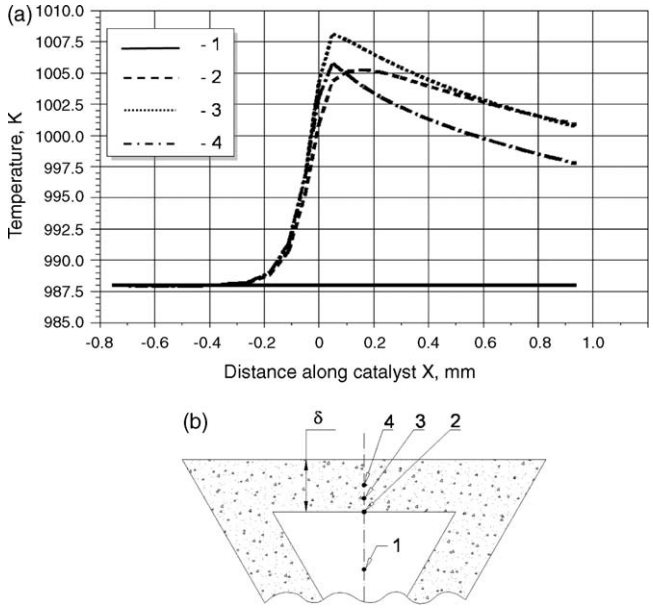

Fig. 3. Temperature profiles along the catalyst fragment (a) for the points 1–4 in the cross-section (b).

of low reagent concentrations and chosen thermostat temperature.

In Fig. 3 the calculated local temperature profiles along the reactor length are given for the region before and inside the channel. That is the zone of maximal changes of the temperature. The axial section of catalyst wall through the middle point of the side of the triangle in cross-section of the fragment is considered (see Fig. 3b). The local profiles correspond to the axis of the reactor (curve 1), middle point at the wall surface of the channel (curve 2), middle point in the wall volume at a distance of $\delta/6$, where δ is the wall thickness (curve 3), and, at last, middle point at a distance of $\delta/2$ (curve 4). The further in the catalyst volume, the nearer is the temperature to the thermostat one. As it was shown by calculated data, the maximal difference between the gas temperature in the flow core and the catalyst temperature does not exceed 20 K, while the difference of temperatures inside the catalyst volume is at most 10 K in the region of highest heating near the channel inlet. Far from the channel inlet the temperature profiles become more smooth, the temperature variation along the whole channel length is bounded within 20 K as well. Thus, for the conditions under consideration the catalyst volume is nearly isothermal.

3.2. Gas flow velocity distribution

The velocity distribution of the reacting gas flow through the catalyst channel under the conditions of the catalytic reaction was analyzed. In Fig. 4, the three-dimensional distribution of the gas velocity in the reactor at several cross-sections of the channel is presented. The cross-sections are taken uniformly with the distance of Δx = 2 mm; the first corresponds to the channel inlet (x = 0), while the last, to the outlet (x = 10 mm). The gas consumption was 18 l/h or 2 m/s (SPT). The aerodynamic conditions in the tube reactor under study are significantly inhomogeneous:

- Near the inlet of the channel, the stream narrows. This causes the velocity field to change in front of the fragment over the distance up to one channel diameter.
- Inside the channel, the flow distribution over the cross-section changes permanently as well. The formation and growth of the boundary layers occur at the walls and especially near the channel edges. The effective open area of the channel narrows, and the flow speeds up in the central part of the cross-section.
- After the channel outlet, a jet stream mixing occurs over the whole cross-section of the reactor; therefore, the maximum axial velocity decreases. Moreover, a reverse-flow and even vortices near the back face of the fragment can appear.

Note that near the channel corners there is a decrease of the gas velocity and, as a consequence, some lowering of the reaction rate too. The "radial" components of the flow velocity are also rather small at the points inside the channel (far from the inlet).

It is possible to estimate the effect of the temperature and chemical reaction on the gas flow velocity distribution. As it was seen from Fig. 3, the gas temperature variation is at most 17 K, which means that the gas density change does not exceed 2%. Taking into account the low concentrations of reagents and stoichiometry of reactions (1) and (2), it can be concluded that the effect of the reaction mixture composition is also insignificant.

The spatial profiles of gas velocity were also obtained for the catalyst channel of 20 mm length. It was shown that they are essentially inhomogeneous as in the case of 10 mm fragment, though the changes become more smooth in the second half of the channel. Thus, even 20 mm length of the channel is insufficient for the flow stabilization.

The above results show that, for conditions under study, there is no flow stabilization over the whole channel length, i.e., we do not observe similar stream-patterns at different cross-sections. The most intensive changing and mixing of the gas streams appear near the channel inlet. Here, the transverse components of the velocity are high and even comparable with the maximal axial velocity in the flow core. That is why the highest local heat and mass transfer rates (between the catalyst surface and the gas flow) are expected to appear in this part of the channel.

3.3. Interphase mass transfer rates

The studies of local heat and mass transfer rates between the channel walls of the catalyst monolith and the reacting gas flow were performed and the parameters of interphase mass transfer were determined on the base of the data on heat transfer rate according to the similarity of the processes. For that, the detailed distributions of local Nusselt and Sherwood numbers were computed over the catalyst surface. Such a distribution of the relative mass interphase exchange coefficient (i.e., the ratio of the local value to the maximal value) is given in the picture of Fig. 5 for the channel of 20 mm length. The feed gas consumption was 36 l/h in this case.

At constant feed consumption the local mass transfer coefficient varies significantly over the channel surface, the difference in the values at some points at the channel walls is up to two orders of magnitude. The maximum is located in the frontal part of the fragment, and, obviously, the values decrease more than five times

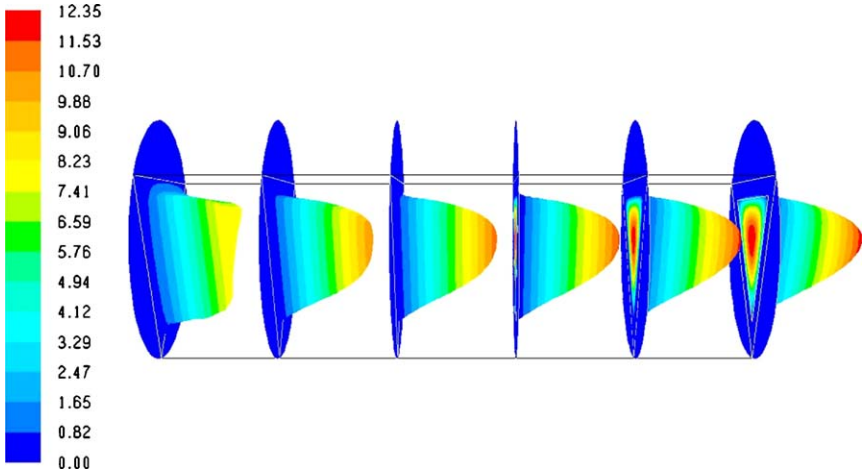

Fig. 4. Distribution of gas velocity over different cross-sections along the catalyst fragment of 10 mm length. The velocity values correspond to the scale on the left.

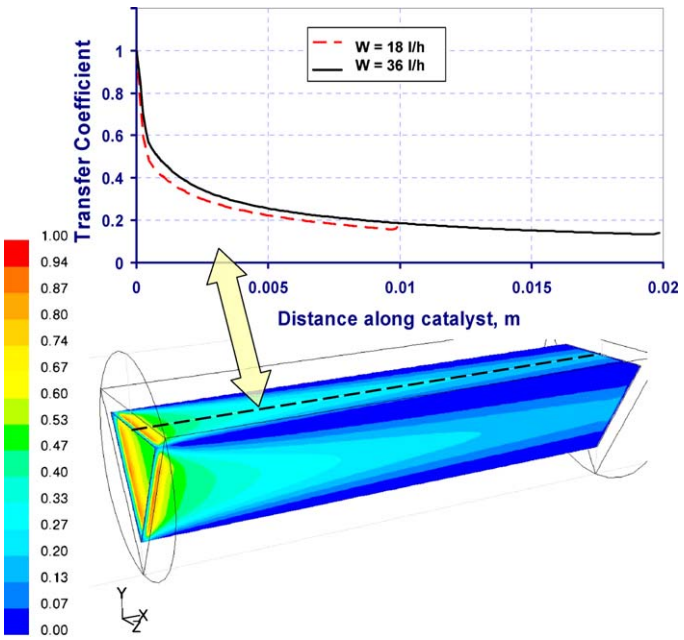

Fig. 5. Relative mass transfer rates over the channel surface.

along the channel towards the outlet. Considering the cross-section of the channel, it was observed that the distribution of the local mass transfer coefficient varies significantly around the perimeter. The highest values are on the middle parts of the sides of the triangle; the regions of minimal interphase transfer rates are located near the edges of the channel due to formation of the boundary layers.

In the plot of Fig. 5, the comparison of the mass interphase exchange coefficients calculated along the symmetry line of the catalyst wall (see the dash line in the picture of Fig. 5) for the feed gas rate of 18 and 36 l/h is also given. The nonlinear dependencies differ from each other in the inlet region of the channel. The decrease of feed consumption results in lowering the interphase transfer rates at a distance of about 10 mm from the inlet, and then the difference becomes insignificant. Note that a rather sharp decrease of the interphase mass transfer is observed in the region of high spatial inhomogeneity of the gas flow.

3.4. Reaction in the porous monolithic catalyst

The local reaction rates in the catalyst volume were determined by Eqs. (1) and (2). To clarify the impact of gas transfer limitation on heterogeneous catalytic reaction, the axial profiles of concentrations, reaction rates and effectiveness factor of the catalyst volume were determined. Similar to Fig. 3, the example of local concentration profiles of methane and oxygen along the reactor length is given in Fig. 6 for the region before and inside the channel. The values were determined at different points of the cross-section (see Fig. 3b, points 1–4).

As for the temperature distribution, there is the zone of sharp changes of the gas composition, after which a smooth decrease follows. The concentrations of reagents in the bulk of the channel and at the gas–solid interface differ considerably, which indicates the influence of the external diffusion. In the catalyst volume the profiles change further in the transverse direction because of the interaction of chemical reaction and internal mass transfer. The impact of gas transfer processes becomes apparent for the concentrations at the frontal interface also. It seems that the lowering of values is observed right before the channel inlet due to back mixing of gas flow.

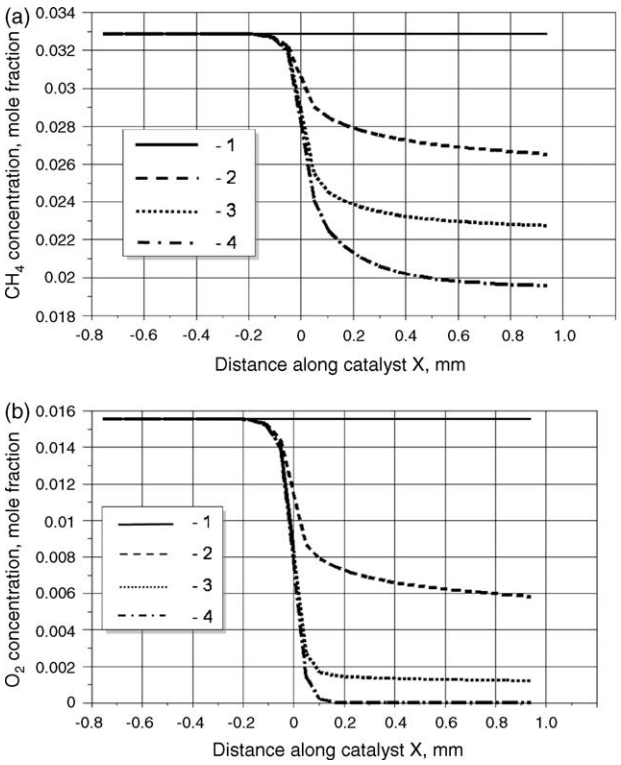

Fig. 6. Profiles of methane (a) and oxygen (b) concentrations along the reactor length for the points 1–4 in the cross-section (see Fig. 3b).

To evaluate in more detail the reaction occurring in the porous volume of the monolith catalyst, a comparison of the volume and surface reaction rates was carried out in the following way. Two average values of each reaction rate were determined along the catalyst: the average rate in the porous honeycomb volume and that on the wall surface. Fig. 7 shows an elementary volume of the catalyst with the cross-section S_0 and length Δx, which was used for finding the averaged values. The averages were calculated over each elementary volume $V_n = S_0\Delta x$ and elementary wall surface of the channel $S_n = P\Delta x$ (i.e., an elementary outer surface of the catalyst; here P stands for the channel perimeter) for a chosen number of cross-sections. The length of an elementary volume Δx dependent on the reaction rate gradients along the catalyst

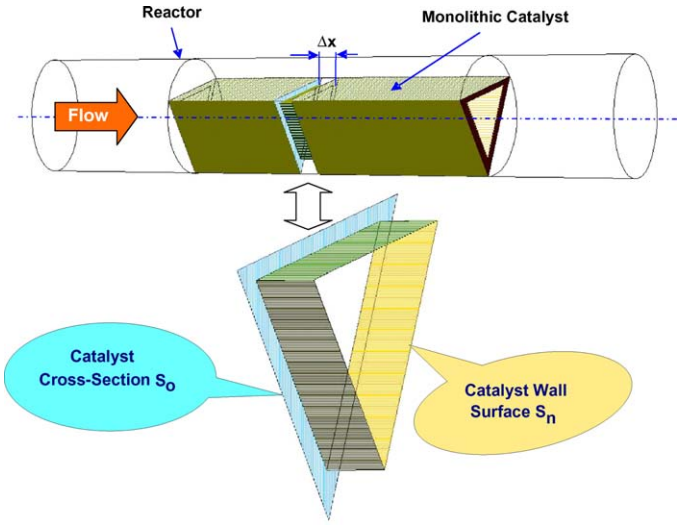

Fig. 7. Elementary surface of the channel wall and catalyst cross-section.

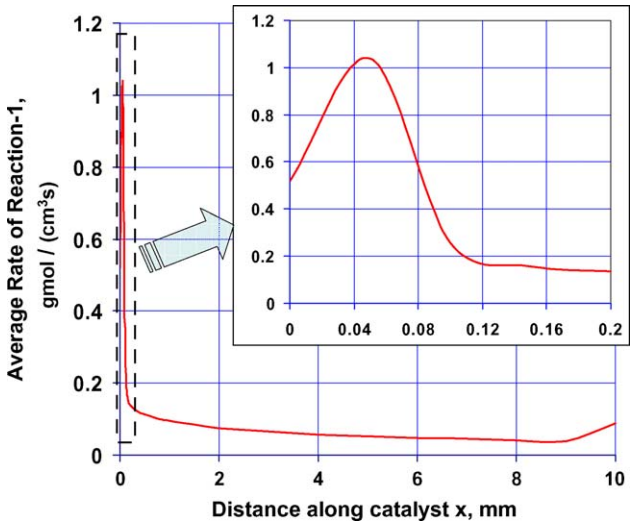

Fig. 8. Methane oxidation rate along the channel length.

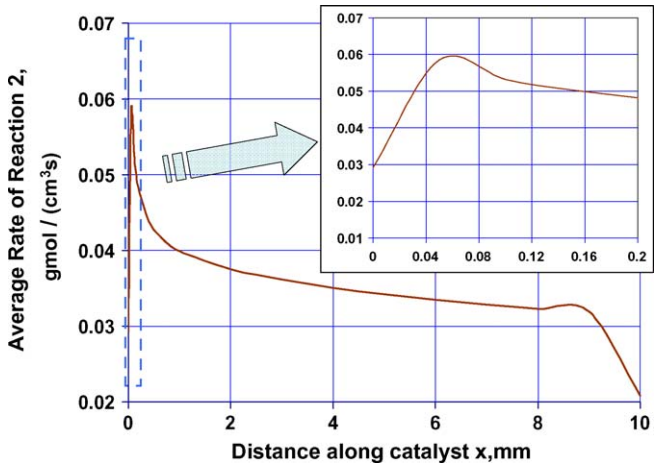

Fig. 9. Profile of the average rate of methane steam reforming along the channel length.

fragment was of 2–8 mesh-steps; as it was mentioned above, the mesh size was determined by the aerodynamic conditions and solution gradients.

The profile of the averaged values of the methane oxidation rate is presented in Fig. 8, the averaging was made over each elementary volume along the porous catalyst structure. The reaction rate rises and passes through the maximum in the catalyst volume near the channel inlet. So, the reaction is the fastest in a small initial part of the channel on a short distance of 0.1–0.12 mm. After the maximum point the oxidation rate falls rather sharply, though the methane and oxygen are present both in the gas and in the catalyst volume; and afterwards the decrease slows down. The latter is obvious and caused mostly by the evident decrease of the reagent concentrations due to transformation of gaseous components under the reaction (see Fig. 6).

Let us estimate the influence of temperature inhomogeneity on the reaction rate at a distance up to 0.12 mm from the inlet, where the sevenfold variation of the volume averaged rate occurs. At the change of the temperature from 1003 to 1008 K, the constant of methane oxidation rate increases by about 5%. Taking into account that all temperature values in this part of the catalyst volume are close to this temperature interval, it can be concluded that the temperature effect on the local reaction rate is insignificant. The local concentration profiles shown in Fig. 6 do not allow us to explain such a behavior of the volume averaged rate also.

The next factor to be considered may be the nonuniform spatial distribution of the gas flow in porous matrix. To understand such a behavior at the reactor inlet, the local distributions of the gas flow velocity and the oxidation rate were constructed over the frontal surface of the catalyst. They show that a sharp increase of the reaction rate in the initial part of the monolith volume may be related with the high rate of penetration of the feed mixture components into the catalyst bulk.

In the area near the interior reactor wall before the catalyst fragment, the flow decelerates and the gas velocity distribution over the frontal surface of the catalyst shows that the gas velocity is the highest near the monolith exterior edges. The rate of the gas flow penetration through the frontal surface into the catalyst volume is much higher than the transverse reagent rates from the gas phase to the internal surface of the porous channel walls. The maximal reaction rate is achieved at a distance of about 0.05 mm from the frontal surface, and the value is almost an order of magnitude higher than the averaged values of conversion rate of the reagents at the other points along the catalyst fragment.

The impact of aerodynamics of the gas flow was also studied for the methane steam reforming for which the catalyst activity is considerably lower as compared to that for the methane oxidation. The reaction rate profile is presented in Fig. 9. On the whole, the reforming rate is significantly lower than the methane oxidation one because of small water concentration in the feed mixture and lower catalyst activity. In spite of this, the impact of the gas velocity distribution on the axial profile of the reaction rate looks similar to that shown in Fig. 8. The reaction rate increases near the channel inlet; thereafter, the value slowly goes down. Note that the methane steam reforming rate distribution is rather smooth as compared to the methane oxidation rate, which is caused by lower values of the reforming rate and, respectively, a weaker influence of the distribution of gas flow velocities in the channel and porous catalyst structure.

Thus, the effects are similar in both cases, and the reaction rates are considerably higher in the area close to the frontal surface in comparison with the values at the points far from the channel inlet. It could be concluded that a similar increase of the reaction rate near the channel inlet can be observed for the other reactions too. As usually, the extent of effect will be due to the relation of the reaction rate and the rate of the reagent transfer from the gas phase to the internal catalyst surface.

3.5. Effectiveness factor for porous catalyst structure

The comparison of the catalyst activity over the porous volume and over the wall surface of the catalyst was carried out for the rate of total methane conversion due to two reactions. The local effectiveness factor η was used to characterize the effect of inhomogeneous distribution of gas flow. This value was defined as the ratio of the reaction rates r_V and r_S averaged over the volume and the surface of the monolith catalyst as follows:

$$\eta = \frac{r_V}{r_S}, \qquad r_V = \frac{1}{V_n}\int_{V_n}(r_1 + r_2)\,dV_n, \qquad r_S = \frac{1}{S_n}\int_{S_n}(r_1 + r_2)\;dS_n.$$

Here r_1 and r_2 are the local values of the reaction rates of methane oxidation (1) and methane steam reforming (2), V_n is the volume, while S_n stands for the channel surface area of this volume.

Fig. 10 presents the correlation between the averaged rates along the channel. At the initial part, the effectiveness factor for methane conversion is above unity, and thereafter it lowers. The profile of the effectiveness factor along the channel length looks like the dependencies of the averaged reaction rates in the volume along the catalyst length (see Figs. 8 and 9). This similarity is caused by the fact that the rates r_S averaged over the surface of the

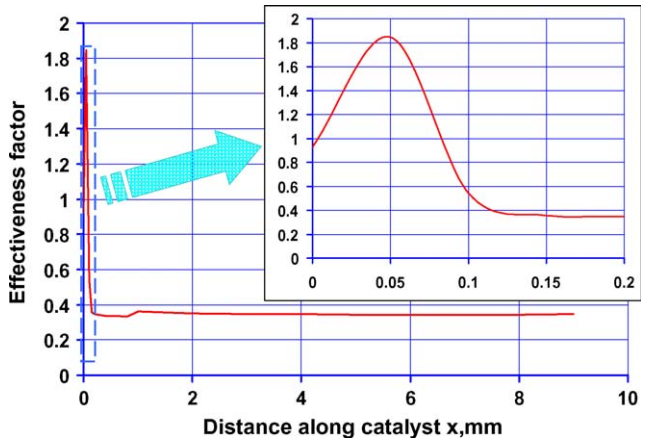

Fig. 10. Effectiveness factor of the catalyst volume for the methane conversion rate.

catalyst walls decrease monotonically along the whole channel length, which was seen from the simulation results.

As it was shown above, the temperature inhomogeneity has no significant influence on the reaction rate distribution on porous matrix. The values of surface temperature lie also in the range considered above; so, the temperature effect on the effectiveness factor is insignificant, too.

It was discussed before that, at the initial part, the feed components penetrate into the catalyst volume through the frontal surface, which can lead to a higher reaction rate inside the catalyst in comparison with that on the wall surface. Correspondingly, the effectiveness factor can become above unity in this part. The difference of the transfer rates of the gas components to the inner surface of the porous structure at the initial part of the monolith (both through the frontal surface of the particle and the wall surface) and far from the channel inlet (only through the wall surface of the channel) influences strongly the effectiveness factor. For conditions under consideration, far from the channel inlet the transport of the reacting species only through the channel wall surface and the sequential mass transfer inside the pores are rather slow, and the local effectiveness factor is less than unity. These data and the concentration profiles show that the methane conversion depends on two processes: the motion of reagents from the gas phase to the channel wall and mass transfer inside pores of the catalyst matrix.

Thus, the studies carried out allow us to conclude that the convective reacting flow going through the frontal surface of the monolith increases significantly the rate of reagent transfer to the active inner surface of the catalyst, and the reaction rates near the frontal surface are higher than on the channel wall surface, and therefore, in this part of the monolith, the effectiveness factor is much higher than unity.

4. Conclusion

In the paper, the studies of the mass transfer in a honeycomb catalyst with triangular channels and reactions occurring inside the porous catalyst structure are presented. The processes in a tube reactor with the honeycomb catalyst fragment in the form of a separate channel are considered.

Computational tools for the numerical simulation of reactive flow were developed using the Fluent software and applied to a three-dimensional model of the heterogeneous catalytic system. The model proposed accounts for the permeability of the catalyst porous structure for the gas flow. The spatial distributions of reacting gas flow, the rates of local mass transfer between channel walls and gas flow, as well as the impact of transfer processes on a catalytic reaction were studied. The reactions of deep oxidation and steam reforming of methane are considered as model reactions.

It was shown that the reacting flow is not stabilized over the whole channel length under studied conditions. The most intensive changing and mixing of the gas streams appear near the channel inlet, which causes the highest local rates of interphase exchange processes. At constant feed consumption, the difference of the local rates over the channel surface is up to two orders of magnitude.

To evaluate the reaction occurring in the porous volume of the monolith catalyst, the comparison of the reaction rates averaged over the catalyst volume and over the channel wall surface was carried out and the local effectiveness factor was determined. It was found that the effectiveness factor of the catalyst has a high maximum near the channel inlet because the feed components penetrate into the catalyst volume through the frontal surface, which leads to a higher reaction rate inside the porous catalyst in comparison with that on the wall surface.

Acknowledgement

The authors are grateful to the reviewers for helpful and valuable discussion.

References

[1] A. Cybulski, J.A. Moulijn (Eds.), Structured Catalysts and Reactors, Marcel Decker, New York, 1998.
[2] R.M. Heck, S. Gulati, R.J. Farrauto, Chem. Eng. J. 82 (2001) 149.
[3] Th. Giroux, Sh. Hwang, Y. Liu, W. Ruettinger, L. Shore, Appl. Catal. B: Environ. 55 (2005) 185.
[4] V.A. Sadykov, S.N. Pavlova, R.V. Bunina, G.M. Alikina, S.F. Tikhov, T.G. Kuznetsova, Yu.V. Frolova, A.I. Lukashevich, O.I. Snegurenko, N.N. Sazonova, E.V. Kazantseva, Yu.N. Dyatlova, V.V. Usol'tsev, I.A. Zolotarskii, L.N. Bobrova, V.A. Kuz'min, L.L. Gogin, Z.Yu. Vostrikov, Yu.V. Potapova, V.S. Muzykantov, E.A. Paukshtis, E.B. Burgina, V.A. Rogov, V.A. Sobyanin, V.N. Parmon, Kinet. Catal. 46 (2005) 227.
[5] R.D. Hawthorn, AIChE Symp. Ser. 70 (137) (1974) 428.
[6] R.K. Shah, A.L. London, Laminar Flow Forced Convection, Academic Press, New York, 1978.
[7] A. Cybulski, J.A. Moulijn, Catal. Rev. -Sci. Eng. 36 (2) (1994) 179.
[8] E. Tronconi, P. Forzatti, AIChE J. 38 (1992) 201.
[9] A. Noskov, Kinet. Catal. 46 (2005) 414.
[10] L.L. Raja, R.J. Kee, O. Deutschmann, J. Warnatz, L.D. Schmidt, Catal. Today 59 (1–2) (2000) 47.
[11] O. Deutschmann, R. Schwiedernoch, L.I. Maier, D. Chatterjee, Stud. Surf. Sci. Catal. 136 (2001) 251.
[12] S. Tischer, Ch. Correa, O. Deutschmann, Catal. Today 61 (2001) 57.
[13] S. Tischer, O. Deutschmann, Catal. Today 105 (2005) 407.
[14] V. Sadykov, S. Pavlova, Z. Vostrikov, N. Sazonova, E. Gubanova, R. Bunina, G. Alikina, A. Lukashevich, L. Pinaeva, L. Gogin, S. Pokrovskaya, V. Skomorokhov, A. Shigarov, C. Mirodatos, A. van Veen, A. Khristolyubov, V. Ulyanitskii, Stud. Surf. Sci. Catal. 167 (2007) 361.
[15] G. Groppi, A. Belloli, E. Tronconi, P. Forzatti, Chem. Eng. Sci. 50 (1995) 2705.
[16] S. Pavlova, N. Sazonova, V. Sadykov, S. Pokrovskaya, V. Kuzmin, G. Alikina, A. Lukashevich, E. Gubanova, Catal. Today 105 (2005) 367.
[17] Fluent, Version 6.1, Fluent Inc., Lebanon, New Hampshire, 2003.
[18] D.L. Trimm, C.-W. Lam, Chem. Eng. Sci. 35 (1980) 1405.
[19] I. Tavazzi, A. Beretta, G. Groppi, P. Forzatti, Stud. Surf. Sci. Catal. 147 (2004) 163.